JACS
JOURNAL OF THE AMERICAN CHEMICAL SOCIETY

Article

pubs.acs.org/JACS

Unusually Stable Hysteresis in the pH-Response of Poly(Acrylic Acid) Brushes Confined within Nanoporous Block Polymer Thin Films

Jacob L. Weidman,[†] Ryan A. Mulvenna,[‡] Bryan W. Boudouris,[‡] and William A. Phillip*[,†]

[†]Department of Chemical and Biomolecular Engineering, University of Notre Dame, Notre Dame, Indiana 46556-5637, United States
[‡]School of Chemical Engineering, Purdue University, West Lafayette, Indiana 47907, United States

Supporting Information

ABSTRACT: Stimuli-responsive soft materials are a highly studied field due to their wide-ranging applications; however, only a small group of these materials display hysteretic responses to stimuli. Moreover, previous reports of this behavior have typically shown it to be short-lived. In this work, poly(acrylic acid) (PAA) chains at extremely high grafting densities and confined in nanoscale pores displayed a unique long-lived hysteretic behavior caused by their ability to form a metastable hydrogen bond network. Hydraulic permeability measurements demonstrated that the conformation of the PAA chains exhibited a hysteretic dependence on pH, where different effective pore diameters arose in a pH range of 3 to 8, as determined by the pH of the previous environment. Further studies using Fourier transform infrared (FTIR) spectroscopy demonstrated that the fraction of ionized PAA moieties depended on the thin film history; this was corroborated by metal adsorption capacity, which demonstrated the same pH dependence. This hysteresis was shown to be persistent, enduring for days, in a manner unlike most other systems. The hypothesis that hydrogen bonding among PAA units contributed to the hysteretic behavior was supported by experiments with a urea solution, which disrupted the metastable hydrogen bonded state of PAA toward its ionized state. The ability of PAA to hydrogen bond within these confined pores results in a stable and tunable hysteresis not previously observed in homopolymer materials. An enhanced understanding of the polymer chemistry and physics governing this hysteresis gives insight into the design and manipulation of next-generation sensors and gating materials in nanoscale applications.

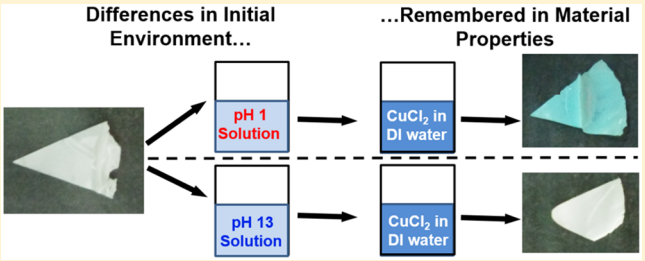

INTRODUCTION

Stimuli-responsive materials are a major field of materials science, and their impact continues to burgeon as their ability to provide a real-time response to changes in their environment (and, thus, provide on-demand sensing information) can be used to control processes in a ready manner.[1] For instance, environmental stimuli that have been shown to produce responses in materials include changes to the relative basicity or acidity (i.e., pH),[2−4] temperature,[5−7] or the presence of specific chemicals.[8,9] These stimuli-responsive materials generally follow a reversible, one-to-one relationship between the environment quality and the material property. For example, for a given pH, the material will correspondingly have a given property, regardless of whether the material was at a higher or lower pH previously. However, in some cases, which may be extremely useful, materials display hysteretic properties, where multiple states of the material can exist in a single environment depending on the history of the material.[10−15] Polymeric materials that display a hysteresis in response to external stimuli may allow for the further development of ionic circuits for use in numerous applications, including smart drug delivery systems and point-of-care diagnostics.[16] This type of hysteretic response to environmental stimuli is rarely reported in polymeric membranes, which tend to display reversible responses to external stimuli. The ability to remember the previous conditions is typically a short-term effect that fades as time passes and the material reaches its equilibrium state,[11−15] and it is exceedingly rare for a material to display a hysteresis that does not decay with sufficiently long periods of time.[10] Conversely, we demonstrate here that when poly(acrylic acid) (PAA) moieties are confined at a high density within the nanopores of a self-assembled block polymer thin film, they exhibit an unusually stable and persistent hysteresis in their response to pH.

In more traditional cases, the nature of the material response depends on the complex interactions between the material and it surroundings. For many weak polymer electrolytes, which have reversible pH-responses, the equilibrium between the ionized and neutral forms of the polymer is determined by the pH of the solution.[17−23] The induced electrostatic interactions along the chain then play a major role in the final conformation of the polymer, which also has to balance the entropic forces that can inhibit the chains from attaining the most extreme extended conformations. The interplay between these two energies results in polymeric materials that have relatively small

Received: February 12, 2016
Published: May 12, 2016

DOI: 10.1021/jacs.6b01618
J. Am. Chem. Soc. 2016, 138, 7030−7039

average sizes for neutral chain conditions and relatively large average size in conditions that promote ionization.[24] However, in the presence of additional attractive enthalpic interactions, the material response can be impacted in a complex manner that may yield multiple stable states at a single environmental condition. One such interaction is the formation of ionic cross-links for materials where multiple oppositely charged chemical moieties are present.[10] Another is the formation of hydrogen bonds, which can happen in homopolymers containing acidic hydrogens as part of a carboxylic or amide group.[25,26] For instance, we demonstrate here that PAA can be manipulated into high density configurations that display this complex behavior through the self-assembly and nonsolvent induced phase separation (SNIPS) method of membrane casting of block polymers.

Casting via the SNIPS method generates thin films with self-assembled nanopores from dissolved block polymers that contain moieties with significant chemical dissimilarities.[27−30] During the casting, sufficient evaporation from the top layer of the drying thin film concentrates the block polymer at the film−air interface, increasing the interactions between the unique moieties of the block polymer chains and eventually favors the formation of distinct domains of separate chemistries on the nanometer scale.[27−29] The final structure of these domains is highly dependent on the block polymer chemistry, composition of the block polymer, and the conditions used during the casting process.[31,32] For many materials that are studied for water filtration applications, the preferred configuration is that of cylindrical domains aligned perpendicular to the membrane surface, resulting in pores that allow flow though the membrane.[3,33−35] This nanoporous thin film has been used as a membrane when a polyisoprene-*b*-polystyrene-*b*-poly(acrylic acid) (PI-PS-PAA) triblock polymer was cast from solution.[36] The pore-lining PAA moiety has been shown to be pH-responsive and have a high enough density that it competes with other copper binding materials as a metal adsorber.[37] This high density of PAA chains confined within the nanoscale features of the membrane allows for hydrogen bonding under favorable pH conditions, as well as limited conformational freedom for the polymer chains. These factors, in combination with the pH-dependent ionization, allow it to have a hysteretic response to changes in environment.

In this current study, PI-PS-PAA-based thin films containing nanoscale pores lined with the poly(acrylic acid) (PAA) moiety were fabricated. These thin films were used as membranes, and they displayed a pH-response that changed the size of the nanoscale pores when they were challenged with a variety of aqueous solutions, as measured in permeability experiments. Unlike most materials that have a reversible pH response, the membranes were shown to have hysteretic permeabilities, with the value of the hydraulic permeability under DI water conditions differing by a factor of 6−8 times difference depending on whether the membrane had previously been in a basic or acidic solution. The hysteresis was consistently repeatable and a long-lived phenomenon. The electrostatic properties of the materials also displayed this unique dependence on environmental history, as did their performance as metal adsorbers. The deviation from a reversible pH response was attributed to the metastable hydrogen bond network of PAA formed under acidic conditions, which allowed the membrane material to retain information about the history of the membrane conditions. The elucidation of this unusually long hysteretic phenomenon provides significantly deeper insights into the physics of these materials and how to manipulate the chemistry, geometry, and environmental conditions of nanoporous polymer thin films in order to generate next-generation sensors[38] and gating materials.[39]

RESULTS AND DISCUSSION

Hysteresis in the Physical Properties of Nanoporous Block Polymer Membranes. The self-assembled, nanoporous membranes used here were generated following the procedure described previously.[36] In brief, the polyisoprene-*b*-polystyrene-*b*-poly(*N*,*N*-dimethylacrylamide) (PI-PS-PDMA) block polymer was synthesized via a reversible addition−fragmentation chain transfer (RAFT) polymerization.[40,41] Subsequently, the isolated PI-PS-PDMA was dissolved in organic solvents and cast into a nanoporous thin film through the SNIPS method. A subsequent reaction of the membrane in a 6 M hydrochloric acid bath converted the PDMA block to a PAA functionality, which resulted in the PI-PS-PAA structure shown in Figure S1a. The PDMA block that had lined the pore walls was fully converted to PAA, resulting in a surface like that shown in Figure S1b, where the PI and PS blocks (represented with red in the cartoon) are the matrix of the membrane, while the PAA (shown by the blue entities) is the moiety that lines the pore walls. Following the functionalization reaction, the membrane surface retained its high density of consistently sized pores, as shown by the SEM micrograph in Figure S1c. Because the PDMA moieties, which are subsequently converted to PAA moieties, are introduced during the synthesis of the block polymer precursor we can confine PAA brushes within the nanopores of thin films cast using the SNIPS method at higher densities than can be achieved using standard grafting-to or grafting-from methodologies. Estimates of this density suggest it is two to three times larger than the densities reported for other methods of introducing polymers onto surfaces.[42,43] It is likely that this high surface density of polymer chains is critical to the hysteretic behavior discussed in this work.

In addition to directing the assembly of nanoscale pores on the membrane surface, the SNIPS method generates an asymmetric structure with large open channels beneath the nanoporous active layer. The large openings in this underlying support layer provide little resistance to flow compared to the active layer, which provides the majority of the resistance due to its small pores. The flux of solution through the membrane is a function of the applied pressure and the hydraulic permeability, as shown in eq 1.

$$J_w = L_p \times \Delta P \tag{1}$$

Here, J_w is the volumetric flux of the permeate through the membrane, ΔP is the applied pressure, and L_p represents the hydraulic permeability of the membrane.[44] For a membrane with a collection of cylindrical pores, the Hagen−Poiseuille equation can be used to calculate the hydraulic permeability, as shown as eq 2, which has a dependence on the pore diameter (D) to the fourth power.

$$L_p = \frac{N_p \pi D^4}{128\,\mu \mathrm{L}} \tag{2}$$

Here, N_p is the areal pore density of the thin film, μ represents the viscosity of the solution, and L represents the length of the pore. Thus, changes in the pore diameter modify the overall permeability of the membrane, or alternatively, observed

DOI: 10.1021/jacs.6b01618
J. Am. Chem. Soc. 2016, 138, 7030−7039

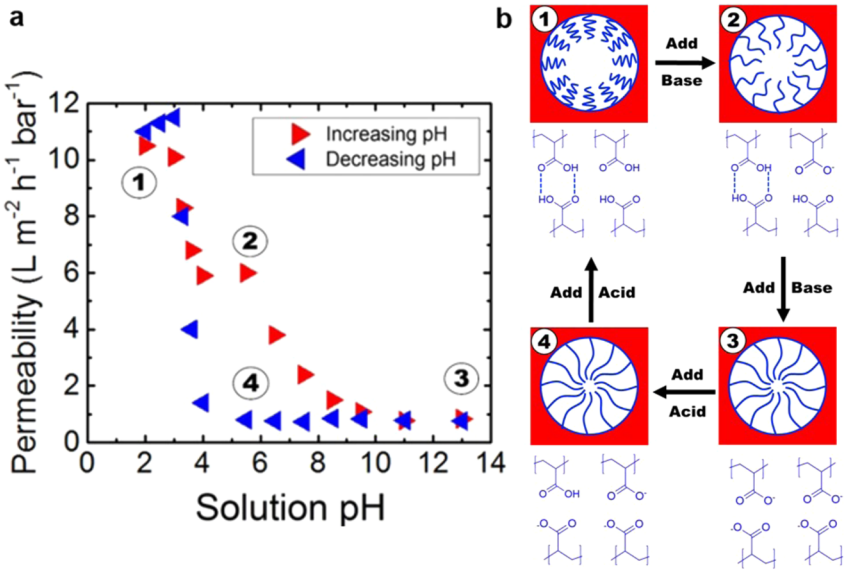

Figure 1. Membrane permeability displays a hysteretic dependence on pH. (a) The hydraulic permeability of a PI-PS-PAA block polymer-based membrane as a function of the solution pH. The membrane was fabricated from the PI-PS-PDMA-44 block polymer sample. Two series of experiments were implemented. First, a membrane began in a pH = 1.0 solution, and its permeability was measured as the membrane was exposed to solutions of incrementally higher pH (red symbols); this is referred to as increasing pH. Second, a membrane began in a pH = 13.0 solution and the permeability was measured as the membrane was exposed to solutions of incrementally lower pH (blue symbols); this is referred to as decreasing pH. (b) Schematic diagrams of the pore structure and PAA conformation corresponding to the four points noted in Figure 1a. The PI and PS block segments form the matrix of the membrane, and are represented as the red region surrounding the pore in the illustration. The PAA chains that line the pore walls are represented in blue. (1) In a pH 2.0 solution, the PAA chains are not extended, resulting in a pore with a relatively large diameter. The carboxylic acid groups of the PAA are protonated and are capable of forming hydrogen bonds with another PAA moiety. (2) After addition of a pH 5.5 DI water solution, some of the PAA repeat units are deprotonated resulting in the PAA chains extending slightly and decreasing the pore size. Some of the PAA repeat units remain hydrogen bonded to their counterparts, which prevents the full extension of the PAA brushes. (3) In a pH 13.0 solution, most of the PAA repeat units are deprotonated and electrostatically repel one another, which results in highly extended chain conformation that reduces the pore diameters. (4) In DI water (pH = 5.5) after exposure to a basic solution, most of the PAA groups remain deprotonated, and the pores retain a very small diameter. The process is repeatable and reversible.

changes in membrane permeability suggest corresponding changes in the pore diameter.

The hydraulic permeabilities of the PI-PS-PAA membranes were measured in stirred cell experiments (see the Supporting Information for the full experimental procedure). Solutions of varying pH were added to a cell containing a 1-in. diameter circular membrane sample. The solutions were prepared at different pHs by dilution of the following acids or bases with DI water: hydrochloric acid (pH 1.0−3.0), citric acid (pH 3.3−5.0), tris(hydroxymethyl)aminomethane (pH 6.5−9.5), and sodium hydroxide (pH 10.5−13.0). A nitrogen gas line was used to apply pressure to the cell in order to push the solution through the membrane. The output of the membrane testing device led to a vial on a scale so that the mass of solution permeated was readily measured as a function of time. The volumetric flux of water through the membrane was determined by dividing the slope of the accumulated mass versus time data by the area of the membrane and the density of water. Dividing this measured flux by the pressure applied (i.e., ΔP) yielded the permeabilities displayed in Figure 1a.

At the beginning of the experiment, with the membrane exposed to a pH 2.0 solution (corresponding to Point 1 in Figure 1) for 2 h, the membrane permeability was 10.9 L m^{-2} h^{-1} bar^{-1}. Following this, solutions of incrementally higher pH were added to the stirred cell, and left to equilibrate with the membrane for ∼20 min. The experiments began and permeated a total of ∼2 mL for each data point over a timespan ranging from 0.5 to 12 h, and the corresponding permeabilities were measured. The results of these measurements, which are denoted by the red triangles in Figure 1, were executed with the solution pH changing as shown (i.e., moving from left to right in Figure 1). The permeability decreased between pH 3.0 and pH 4.0, then remained constant at ∼6.1 L m^{-2} h^{-1} bar^{-1} in DI water at pH 5.5 (Point 2, Figure 1). Further increasing the pH resulted in a gentle decrease in permeability until the solution pH was around pH 9.5 where the permeability neared its lowest value of 0.9 L m^{-2} h^{-1} bar^{-1}. The permeability remained constant at this value through a pH of 13.0.

Beginning from a pH 13.0 solution (Point 3, Figure 1) and decreasing the pH, the permeability values matched that of the increasing pH experiments through a pH of 9.5. However, the permeability values showed clear hysteresis beyond this point, as the permeabilities below this pH remained near 1.3 L m^{-2} h^{-1} bar^{-1} through to a pH of 4.0, including DI water at pH 5.5 (Point 4). Below pH 4.0, the permeability began to rise sharply. At a solution acidity of pH ∼ 3.2, the permeability value for the experiments executed with solutions of decreasing pH rejoined the permeability values from the curve for experiments conducted with increasing pH. For solutions with a pH below this value through a solution pH of 2.0, the measured permeabilities matched. It is noted that between the pH values of 3.2 and 8.5, the permeabilities did not match between the two curves. This clear hysteresis in the permeability with respect to pH is of significant interest as controlling the previous pH conditions of the solution to which the membrane was exposed will impact the permeability in the near DI water (i.e., typical operating) conditions. Continued experiments in both directions showed the trend was repeatable and

DOI: 10.1021/jacs.6b01618
J. Am. Chem. Soc. 2016, 138, 7030−7039

consistent. Furthermore, this phenomenon was observed across membranes fabricated from several block polymer samples. That is, the PI-PS-PAA material consistently produced nanoporous thin films that can have different permeabilities at a single pH value depending on whether it was previously in a high or low pH solution, and this phenomenon is unique relative to other reports of PAA in the literature.[17,45−47]

Therefore, this unusual phenomenon must be related to the exclusive chemistry of the triblock polymer and the confined geometry afforded by membranes fabricated using the SNIPS casting procedure.

The observed changes in permeability result from changes in the diameters of the pores within the active layer of the membrane, as we have demonstrated previously.[36] These are, in turn, determined by the physical and chemical interactions between the repeat units of the PAA chains that line the pore walls. Because these repeat units contain a carboxylic acid moiety, their interactions with the surrounding solution may cause them to protonate or deprotonate, depending on the solution pH. At pH 1, the chains are highly protonated, as depicted in Figure 1b. Protonated carboxylic acids, including PAA, have the ability to form hydrogen bonds with other carboxylic acids (e.g., repeat units along the same chain or with units on neighboring PAA chains).[10] This results in the possibility of some PAA units forming a hydrogen-bonded network, as shown schematically in the top left panel of Figure 1b. In turn, the resulting pore has a relatively large diameter due to the collapsed state of the uncharged PAA chains, which corresponds to the highest permeabilities observed in Figure 1a. Increasing the solution pH by adding a DI water solution deprotonates some PAA repeat units that are not involved in hydrogen bonds, as shown in the top right panel of Figure 1b. Many hydrogen bonds remain intact, while the partial charging of the free (i.e., repeat units not associated with hydrogen bonds) PAA units results in the extension of the PAA chains toward the center of the pore, decreasing the observed permeability to nearly half of that of the acidic state.

Adding a basic solution (pH 13.0) results in the deprotonation of almost all of the PAA units, inducing a greater extension of the PAA chains toward the center of the pore due to electrostatic repulsion between the repeat units of like charges. The electrostatic repulsion between PAA units is strong enough to disrupt the hydrogen bonded network. The ionized PAA chains swell to the point that the pores are nearly closed off in the base state, as shown by the bottom right panel of Figure 1b, which is plausible given the radius of gyration of the PAA block is ∼25 nm and the dry state radius of the pores is ∼20 nm. This, combined with the high surface density of PAA (between 0.5 to 1 chains nm^{-2}) along the pore walls, results in the pore volume being nearly completely occupied by PAA chains and a near zero permeability. Adding a more acidic DI water solution to the membrane results in the reprotonation of some PAA units, though still only a small fraction. The electrostatic interactions that are still present dominate the PAA chain response and cause the pore to retain its nearly closed state, as displayed in the bottom left of Figure 1b. Addition of the original acidic solution reprotonates the chains and induces hydrogen bonding, returning the system to the state shown schematically in the top left panel of Figure 1b. This cycle can be repeated with the same states achieved in a consistently reproducible manner.

The effects of solution pH on the permeability of membranes with pores lined by PAA brushes have been investigated in several prior studies.[17,45−47] However, in these prior investigations no hysteretic behavior was noted for the PAA-lined membranes. Rather, the permeability of the membrane displayed a reversible response to pH with no dependence on the previous state of the membrane. Above the pK_a of PAA, the chains were deprotonated and swelled. Below the pK_a, the PAA units became neutral (i.e., protonated) and assumed a less extended conformation. While the pK_a value of acrylic acid monomers is 4.3, the pK_a value of homopolymer PAA dissolved in a bulk solution is higher (6.5) due to charge regulation (i.e., the repulsive electrostatic interactions along the polymer chain driving the acid−base equilibrium toward protonated PAA repeat units).[18,48] Additionally, the pK_a value of polymers in confined spaces may deviate slightly, in the case of a weak acid to an even higher value, as the excluded volume interactions increase the unfavorable interaction energies of the ionized units.[18,49] It is assumed that the effective pK_a of the PAA in this system lies between the sharp changes in permeability observed at pHs of 3.4 and 7.5, though the actual value remains unclear due to the hysteretic behavior.

Hysteretic events have been observed in the pH response of some membranes and other polymeric materials.[10,12−15] However, it is extremely rare for a material to display long-lived hysteretic swelling; for instance, this has been reported in a gel that contained both positively and negatively charged moieties, but not in a porous membrane.[10] Rather, almost all experiments with hysteretic films or membranes demonstrated that the hysteresis was kinetic in nature and, given sufficient time, would disappear.[12−15] The kinetic limitations could be associated with polymer chain relaxation or lack of solvent access to all of the chains within the membrane pores. By allowing sufficient time for polymer chain relaxation, the chains were able to reach equilibrium conformations that are not achieved immediately after changing pH conditions.[12,14] Alternatively, the residual behavior could be a result of needing sufficient permeation of a solution to allow the system to return to equilibrium.[15] The return to equilibrium could be achieved in these cases within seconds to hours of being left to equilibrate. For this reason, permeability experiments on long time scales with DI water solutions were performed on the membranes.

Specifically, membranes were exposed to a pH 1.0 solution, 5 mL of which was permeated through the membrane to ensure that the pore walls throughout the active layer of the membrane achieved equilibrium with the solution. Then the cell was washed several times with DI water and left to soak for 1 h before adding a fresh 10 mL of DI water, and the membrane permeability was measured as a function of time. After 4 mL had permeated, the cell was emptied and a fresh 10 mL of DI water was added. This was repeated until a total of 12 mL had permeated through the membrane. The measured permeabilities are displayed by the red squares in Figure 2. Initially, the permeability decreased over the first 3 mL in the presence of the DI water solution. The pore-lining PAA groups swelled partially during this time as the DI water deprotonated more of the carboxylic acid units as the water permeated though the pores. This value then leveled after 3 mL and remained at the relatively high value of 8.5 L m^{-2} h^{-1} bar^{-1} during the rest of the experiment, which lasted several hours. A similar experiment was performed after the membrane had been exposed to a pH 13.0 solution, with the measured permeabilities shown by the blue circles in Figure 2. The permeability did not change significantly throughout the permeation of 12 mL of DI water

DOI: 10.1021/jacs.6b01618
J. Am. Chem. Soc. 2016, 138, 7030−7039

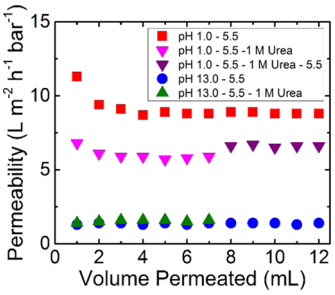

Figure 2. Hysteretic states are long-lived and are affected by the addition of urea. The hydraulic permeability of a PI-PS-PAA block polymer membrane as a function of the volume of DI water permeated. The membrane was fabricated from the PI-PS-PDMA-97 block polymer sample. All measurements were collected using a solution at pH 5.5. Data points represent the average value for each 1 mL of permeate collected. The history of the solution passing across the membrane is summarized in the legend with the terminal entry being the condition used during permeability measurements. A membrane was rinsed with DI water after being exposed to a pH 1.0 solution, then the DI water permeability was measured (red squares). A 1 M urea solution was then added to the stirred cell and the permeability was evaluated (magenta triangles). The cell was then filled with DI water again and the permeability was measured (purple triangles). A membrane that was exposed to a pH 13.0 solution was rinsed with DI water and measured for its DI water permeability (blue circles). This was followed immediately by permeability measurements of a 1 M urea solution (green triangles).

over a period of 10 h. This suggests that the hysteresis is neither kinetically trapped by insufficient relaxation time, nor limited by lack of access of the bulk solution to PAA repeat units within the pores. Rather the membrane remains in long-lived metastable states that have different pore sizes at the same pH.

The approximated pore diameters shown by the cartoons in Figure 1b are based on the observed permeabilities in Figure 1a. These are assumed to be affected greatly by the differences in electrostatic repulsion in the different pH conditions, which is determined by how many of the PAA units are charged. One straightforward way to establish the degree of ionization is through FTIR spectroscopy, which has been shown to display different absorption peaks for the different states of PAA.[18,50,51] Protonated carboxylic acid units absorb at wavenumbers of ~1720 cm^{-1}. This is true for both hydrogen-bonded PAA (1729 cm^{-1}) and free protonated PAA (1712 cm^{-1}), though the observed peaks may be difficult to deconvolute.[51] The deprotonated form of PAA has several absorption peaks, one of which occurs around 1550 cm^{-1}.[18] The relative areas of these characteristic peaks can be used to determine the relative ionization of PAA in membranes under different experimental conditions. Thus, membrane pieces were prepared by soaking them in pH 1.0 or pH 13.0 solutions for at least 1 h, followed by soaking the membranes in a solution prepared at another pH. The solutions used were prepared in the same manner as described above for the permeability experiments. The membranes were left to soak in the solutions of various pH values for 4 h, then pulled from the solution, dabbed with a porous cloth to visual dryness, and vacuum-dried for 20 m.

The samples were vacuum-dried in order to remove water that was present within the hydrophilic pores that would absorb in the range of 1650 cm^{-1}, disrupting the readings of the protonated and deprotonated peaks. A sample Fourier transform infrared (FTIR) spectra of a membrane soaked in a pH 1.0 solution is shown in Figure S2, with the most prominent peak in the plotted range occurring between 1700 and 1750 cm^{-1}.

Four representative FTIR spectra are shown in Figure 3a, and these are labeled 1−4 in order to correspond with the

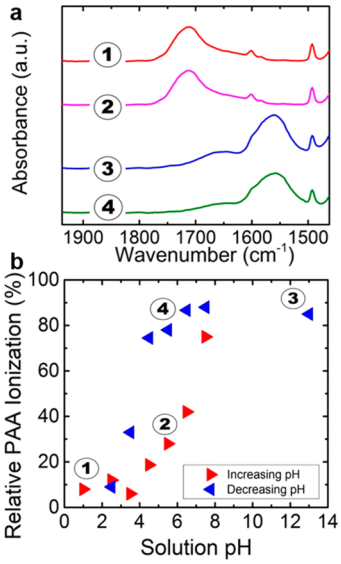

Figure 3. Degree of ionization of PAA shows a hysteretic dependence on pH. (a) FTIR spectra of vacuum-dried membranes after exposure to the four pH conditions labeled in Figure 1a. These conditions are the membrane: (1) exposed to a pH 1.0 solution (red line); (2) soaked in a pH 5.5 solution (magenta line), after exposure to a pH 1.0 solution; (3) exposed to a pH 13.0 solution (blue line); and (4) soaked in a pH 5.5 solution, after exposure to a pH 13.0 solution (green line). The peak at ~1712 cm^{-1} in the red and magenta curves corresponds to protonated carboxylic acids, and the peak at ~1560 cm^{-1} in the blue and green curves corresponds to deprotonated carboxylic acids. (b) The relative degree of ionization of the PAA chains as a function of solution pH. The pH was increased following exposure to a pH 1.0 solution (red triangles) or decreased following exposure to a pH 13.0 solution (blue triangles). The values of percent ionization were determined from the peak areas in the normalized FTIR spectra.

preparation conditions shown in Figure 1. After exposure to a pH 1.0 solution, the resulting FTIR spectrum shown in the red curve and labeled with a 1 displayed a broad peak near the 1720 cm^{-1} wavenumber, suggesting the presence of protonated PAA groups. A membrane that was soaked in pH 1.0 solution followed by DI water, shown by the magenta curve (Trace 2), provided a similar peak in the 1720 cm^{-1} region. This suggests that the PAA chains in these two states are mostly protonated, as was depicted in Figure 1b. Note that it is difficult to determine if the PAA forms hydrogen bonds using this experimental technique due to the potential for overlap of the hydrogen-bonded and free PAA signals. Upon exposure to pH 13.0 solution, the resulting FTIR spectrum shown in blue (Trace 3) displayed a peak near 1550 cm^{-1}, and the acquired FTIR spectrum of a membrane soaked in DI water following the soak in basic solution showed similar absorption, as shown by the green curve with the label 4. This suggests that the PAA groups were mostly deprotonated, as was depicted in Figure 1b. Similar to the permeability measurements in DI water, there was a significant difference in the FTIR spectra of the membranes soaked in DI water after exposure to highly acidic and basic solutions, (magenta and green curves), respectively.

DOI: 10.1021/jacs.6b01618
J. Am. Chem. Soc. 2016, 138, 7030−7039

This difference demonstrates that the ionization of PAA units in DI water is strongly dependent on the previous solution conditions surrounding the membrane.

Additional FTIR spectra were collected for pieces of membranes over a range of pH values, using solutions prepared in the same manner as those described for the permeability experiments. The degree of ionization was observed as the solution pH changed incrementally between the four states shown in Figure 3a. The differences in ionization were quantified using area calculations for the peaks at 1720 and 1550 cm^{-1}, where the fraction of the area under the 1550 cm^{-1} peak divided by the area under both peaks gave the value plotted on the vertical axis for the data in Figure 3b. Samples that were initially soaked in pH 1.0 solution, followed by a solution of a higher pH are shown by the red triangles, which showed a small increase in percent ionization from near 10% at pH 1.0 to around 25% under DI water conditions. The ionization then increased sharply between pH 6.5 and pH 7.5 to near 75% ionization, as more PAA chains were able to deprotonate and attain their equilibrium conformation as per the mechanism proposed above. The blue triangles display the percent ionization for samples that were initially soaked in a pH 13.0 solution before soaking in a lower pH solution. The percent ionization began near 85%, then remained near this value, dropping only to around 75% under DI water conditions. The percent ionization showed a sharp decrease between the pH values of 4.5 and 3.5, before the ionization levels of the membranes agreed with samples initially soaked in acid below a pH of 2.5. The region where the two curves do not lie on top of one another show that a hysteresis in the ionization levels occurs, which matches well with the permeability hysteresis shown in Figure 1. While somewhat counterintuitive, the relatively gradual change over multiple pHs from low to high ionization levels (and vice versa) is consistent with theory for densely packed polymers grafted to a surface.[52] A comparison between the permeability and the percent ionization is also displayed as Figure S3, and it shows a strong correlation between the two metrics. This backs the hypothesis that the observed hysteresis that arises in the physical properties of the block polymer membrane is correlated with the discontinuous change in the electrostatic interactions between the repeat units of the polymer chains. This discontinuous change in the electrostatic interactions is caused by hydrogen bonds between the PAA repeat units preventing some of the repeat units from deprotonating.

Hysteresis in Chemical Properties of Membrane. In addition to controlling the physical properties of the membrane, the ionization of the PAA groups controls the chemical properties of the membranes. One property that relies on ionized PAA repeat units is the adsorption of copper ions, which has been discussed in previous literature.[37,53,54] In our prior studies, membranes that were exposed to a basic solution, and thus had mostly ionized PAA groups, were soaked in $CuCl_2$ solutions in DI water. Copper ions were reversibly adsorbed by the negatively charged PAA units, and the membranes were regenerated with the addition of a pH 1 solution, which shifted the equilibrium to favor protonated PAA repeat units and released the copper ions back into solution. The concentration of copper in the retentate solution and the pH 1 copper regeneration solution were determined via ultraviolet−visible (UV−vis) light spectroscopy, resulting in measured copper uptakes for the membrane under different conditions. In this study, the hysteretic behavior of the copper uptake was assessed in a similar manner. Several 8 mM $CuCl_2$ solutions were prepared at pH values between 1.0 and 7.5 via dilution of hydrochloric acid, citric acid, and tris(hydroxymethyl)-aminomethane (above 8.0 the copper hydroxide may precipitate). Pieces of membrane were soaked in either a pH 1.0 or pH 13.0 solution for at least 30 m, then removed and dipped quickly in a large DI water bath. This was done to remove any residual solution on the membrane before placing them into the 8 mM $CuCl_2$ solutions. The nanoporous thin films were left for 8 h to adsorb copper, then removed and placed in the pH 1.0 solutions to release the bound copper.

The amount of copper bound to the membrane in these experiments was determined from the depletion of copper from the retentate solution and the concentration of the acid wash solution by the characteristic absorption of copper ions at λ = 930 nm. These data are plotted in Figure 4a as a function of the pH of the copper solution. The red data points indicate the membrane pieces that were initially soaked in pH 1 solutions, while the blue data points are membranes initially in pH 13.0 solutions. For the membranes that had soaked in a pH 1 solution, the amount of copper adsorbed was very low, even in the DI water solution, before increasing to near 0.45 mmol g^{-1} at a pH of 7.5. For the membranes soaked in pH 13.0 solutions, the uptake was significantly higher at 7.5, and remained high in DI water, showing a large difference from the uptake after exposure to acid.

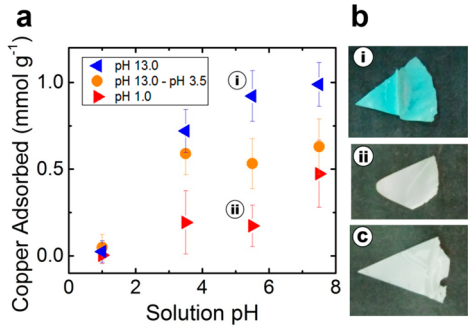

Figure 4. Copper binding in membranes is hysteretic and tunable. (a) The amount of copper adsorbed by membranes exposed to solutions of varying pH. After the membrane was soaked in a copper-free solution of pH-adjusted water [pH 1.0 (red arrows), pH 13.0 (blue arrows), or pH 13.0 followed by pH 3.5 (orange circles)], it was placed in an 8 mM $CuCl_2$ solution at the pH values indicated on the horizontal axis. (b) Photographs of the membrane samples after soaking in an 8 mM $CuCl_2$ solution at pH 5.5. Prior to submerging the membrane in the copper chloride solution, they were (i) soaked in a pH 13.0 solution and (ii) soaked in pH 1.0 solution. Sample (c) is a control membrane that was not exposed to a copper-containing solution.

This can also be observed visually, as shown in Figure 4b, as two pieces of membrane that were soaked in a (i) basic or (ii) acidic solution were added to an 8 mM $CuCl_2$ solution at pH 5.5, then removed and photographed after adsorbing copper. The membrane after exposure to the basic solution appeared blue, while the membrane that was soaked in acidic solution had a similar hue to the membrane not placed in a copper solution (c). Continuing on to lower pH values, for the pieces initially soaked in basic solution, the membrane uptake decreased at pH 3.5, while still at a higher value than the acidic membranes at this pH, then finally matched the pH 1 uptake. The hysteresis in copper adsorption followed a trend

DOI: 10.1021/jacs.6b01618
J. Am. Chem. Soc. 2016, 138, 7030−7039

similar to that which was observed for values of PAA ionization percentage as a function of pH. A comparison is shown in Figure S4, where the PAA percent ionization in the membrane, as measured by FTIR spectroscopy, was compared to the PAA ionization level based on copper uptake at different pH values. These values were calculated using the assumption that a Langmuir isotherm, which is defined by eq 3, holds true for the system,

$$q = \frac{QKC}{1 + KC} \tag{3}$$

where q is the amount of copper adsorbed in mmol g^{-1} membrane, Q is the maximum capacity of copper binding for a given membrane state in mmol g^{-1} membrane, C is the concentration of copper in solution, and K is an equilibrium constant. The concentrations of copper in solution and copper adsorbed on the membrane were known experimentally. Solving the equation at a given condition allowed the value of K to be determined. By assuming that the number of available binding sites arises from the number of negatively charged PAA units, the value of Q determined at any given condition and the fraction of PAA repeat units that are ionized are proportional, allowing for the estimation of the PAA percent ionization based on the copper uptake under each pH condition. These calculations are described in more detail in the Supporting Information. These data are plotted, in addition to the FTIR-measured percent ionizations, in Figure S4. A comparison of the percent ionization levels determined using the two techniques demonstrated a similar trend. This is consistent with Figure S5 where the percent ionization determined from FTIR was compared directly to the copper uptake values. From these data, it can be seen that the observed hysteresis in the electronic state of the membrane also occurs very similarly in the chemical properties of the membrane.

Further studies attempted to determine if the pH values that showed intermediate levels of PAA ionization would display corresponding intermediate levels of copper uptake. This was successfully demonstrated by the experiments detailed in the Supporting Information. Whereby, using careful conditioning of the membrane, the pH-dependent properties could be tuned by controlling the exposure of the membrane to solutions of varying pH. In one specific example, the copper uptake can be trapped at intermediate values, as shown in Figure 4. That is, the orange data points in Figure 4 demonstrated this point and support the assertion that the observed pore sizes strongly correlate with chemical properties.

A final copper uptake experiment was performed, in which membranes that had previously soaked in acidic (pH 1.0) or basic (pH 13.0) solutions were added to scintillation vials containing DI water as before, but left for ∼150 h instead of ∼3 h. The membranes were then removed from the DI water solutions and added to vials of 8 mM $CuCl_2$ to determine the copper uptake. Based on both the depletion of the copper from the feed solution and the amount released in the acid wash, values for the copper uptake were determined. The membrane that was initially soaked in basic solution had a resulting uptake of 0.72 ± 0.05 mmol g^{-1} membrane, while the membrane initially soaked in acidic solution had a resulting uptake of 0.35 ± 0.06 mmol g^{-1}. These values fall just outside the range of the error of the short soak time experiments, but remain distinct from one another. This suggests that unlike other materials that show a short-lived hysteresis on the order of minutes to hours, the PI-PS-PAA membrane displays a hysteresis that endures up to a week in solution, and possibly longer.[12,14]

Hysteresis Arises from the Hydrogen Bonding of PAA. The pores of the nanoporous block polymer thin film show hysteretic and tunable behavior in both physical (i.e., pore size) and chemical (i.e., copper binding) properties, but the cause of the hysteresis is not elucidated merely by the presence of these properties. If the state of the PAA chains that line the pore walls in DI water after exposure to either acidic or basic solution is the local minimum in free energy, a disturbance of the PAA chains from the metastable state may drive the PAA conformation toward to the global minimum in free energy. It has been noted that PAA has the ability to form hydrogen bonds with itself when it is placed in acidic conditions that cause the carboxylic acid moieties to protonate. It is possible that a network of hydrogen bonds may persist in DI water after the membrane was initially exposed to acidic conditions, as shown in Figure 1b. In this case, the DI water does not deprotonate enough PAA repeat units to perturb the system sufficiently to break the network of hydrogen bonds. This results in a metastable state, where the ionization level would be higher if all of the PAA units were free rather than some of them being locked in hydrogen bonds. This keeps the PAA in a more collapsed conformation, resulting in larger pores with less ionization of the PAA units. Because the difference between hydrogen-bonded and free PAA in FTIR spectroscopy is not easily measured, experiments were performed that introduced urea, which can be used as a hydrogen bond disruptor in solution,[55,56] to the nanopores. That is, two membrane pieces were placed in DI water following exposure to an acidic (red) or basic (blue) solution, and they were then evaluated using FTIR spectroscopy (Figure 5a). Similarly, two more pieces were placed in the same conditions followed by soaking in 300 mM urea for 2 h, and then they were evaluated using FTIR spectroscopy. The spectra for the urea-soaked membranes after initially soaking in an acidic solution are displayed in Figure 5a as the magenta curve, with membranes initially soaked in a basic solution shown by the green curve. For membranes initially soaked in a basic solution, the change of the spectra before and after the addition of urea is minimal. However, the change in spectrum for the membrane that was initially soaked in an acidic solution is significant, with a large increase in the degree of ionization. This was further supported by copper uptake experiments shown in Figure 5b, where the amount of copper uptake is plotted against the concentration of urea in the soaking solution before being added to the copper solution. The membranes that had been exposed to urea after exposure to acid showed an increase in copper uptake above 100 mM of urea. This demonstrates that the presence of urea disrupts hydrogen bonds between PAA repeat units, and results in an increase in the degree of ionization of the PAA repeat units.

Urea disrupts the hydrogen bonds between PAA repeat units, which allows more acrylic acid groups to equilibrate with the surrounding solution, resulting in an increase in the ionized form of PAA. This, in turn, increases the magnitude of the repulsive electrostatic interactions between PAA chains, which is expected to cause chain extension, further decreasing pore size, and therefore, the permeability of the membrane. This was established in permeability experiments, immediately following the DI water permeability tests in Figure 2. After the membrane was exposed to acid, followed by DI water, the permeability leveled to a value near 9.0 L m^{-2} h^{-1} bar^{-1}, as shown by the red squares. After the addition of a 1 M urea solution to the cell,

DOI: 10.1021/jacs.6b01618
J. Am. Chem. Soc. 2016, 138, 7030−7039

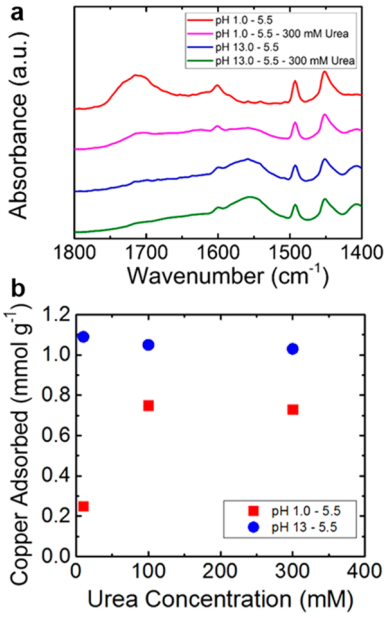

Figure 5. Urea disrupts hydrogen-bonded PAA network. (a) FTIR spectra of membranes exposed to a solution containing urea. After exposure to either an acidic (pH 1.0) or a basic (pH 13.0) solution and subsequent soaking in DI water or DI water then a 300 mM aqueous solution of urea, the membranes were dried under vacuum and analyzed. (b) Copper uptake of membranes after soaking the membranes in solutions of varying urea concentrations (10 mM, 100 mM, 300 mM) after an initial exposure to pH 1.0 (red squares) or pH 13.0 (blue circles). The membranes were removed from the urea solutions and placed in copper solutions at pH 5.5 and left to adsorb copper overnight. A subsequent soak in pH 1 acid released the copper ions, and the copper concentrations of both the retentate and acid solutions were used to determine the amount of copper adsorbed in the membrane.

the permeability decreased and achieved a steady-state value 6.2 L m^{-2} h^{-1} bar^{-1} after 2−3 mL had permeated, as shown by the magenta triangles in Figure 2, which held steady through 8 mL of permeate. To test if the urea solution had only temporarily disrupted the state of the pores, the cell was washed and an additional 10 mL of DI water was added to the cell. The addition of urea after the membrane was exposed to DI water after basic solution resulted in no noticeable change in permeability, as shown by the green triangles. This suggests that the pore size decreases after addition of urea, due to both the breaking of hydrogen bonds that limit the extension of the PAA and the increase in ionization. Breaking hydrogen bonds perturbs the membrane to a state with smaller pores, suggesting that the presence of hydrogen bonds drives the observed hysteretic behavior in the PI-PS-PAA membranes.

Generally in polyelectrolytes a balance between the conformational free energy from entropic considerations and repulsive interactions of the ionized repeat units (which can vary by roughly 200 kJ mol^{-1} for these PAA chains) control the polymer conformation in a reversible manner.[24] However, the energy associated with the formation of a hydrogen bonded network provides a source of deviation from more typical reversible conformational changes. The stability of the hydrogen bonds, which have typical bond strengths of 10−20 kJ mol^{-1}, provides a sufficient decrease in free energy in the system to hold the PAA chains in the protonated form rather than the deprotonated form.[25,26] For an average PAA chain length of 200 units, the hydrogen bonding of ∼10−20% of the units would result in an interaction energy on the same order of magnitude as the repulsive electrostatic forces. As such, a hydrogen-bonded network could reasonably compete energetically with the electrostatic interactions to produce a local minimum in the free energy landscape that prevents the deprotonation of PAA repeat units and polymer extension in DI water after exposure to an acidic solution. The addition of urea is able to partially overcome this barrier due to the breaking of some hydrogen bonds and move the system toward the equilibrium state. However, it is noted that both the decrease in permeability (Figure 2) and the increase in copper uptake (Figure 5b), did not result in values equal to those of the highly ionized (i.e., base exposed) form in DI water. Experiments with urea binding showed that at pH 5.5 residual urea was still present, and did not complete vacate the membrane, until a more basic solution was added. This suggests that the urea is bound within the membrane in DI water and that this prevents it from attaining equilibrium, shown by the blue data at pH 5.5 in both figures. Still, the addition of urea resulted in the disruption of the hydrogen bonded PAA network of the pore walls, which acts as the main driver of the hysteretic response to changes in pH.

Heat was also investigated as a means for disrupting the metastable conformation of the PAA chains within the membrane pores. Membrane sections were soaked in a pH 1 solution, then placed into a vial containing ∼2 mL of DI water. The vial was heated to moderate temperatures (i.e., 40 °C, 55 °C, and 70 °C). Experiments above 70 °C were not executed because the PI-PS matrix material begins to soften at this temperature. After 16 h at the elevated temperature, the vials were cooled in a water bath for ∼5 min. The copper uptake capacities of the membrane sections were quantified as described previously. The results of these experiments, which are displayed in Figure S6, demonstrate that the increased temperature has a negligible effect on the uptake of copper in this system, which suggests that the metastable hydrogen bonded network is not disrupted upon heating to 70 °C. This result is sensible given a comparison of the relative energy within a hydrogen bond (∼10 kJ mol^{-1}) to the energy added upon increasing the temperature of the system (∼0.3 kJ mol^{-1}). The relatively mild heating from 25 to 70 °C (the upper temperature limit for this polystyrene-based membrane system) does not provide sufficient energy to perturb the metastable hydrogen bonded network to the more ionized state.

■ CONCLUSIONS

The chemistry and confined geometry of the weak electrolyte polymer evaluated in this study demonstrates that control over these crucial nanoscale properties leads to tunable behavior of a nanoscale material that has a memory of the previous environment. This hysteretic behavior, which is rarely reported in membrane systems, is possible due to the uniquely high density of PAA chains that line the pore walls of membranes fabricated using the SNIPS method. Nanoporous thin films containing pores with a PAA lining that were exposed to basic solutions followed by DI water resulted in extended, highly charged PAA chains that resulted in low pore diameters and high copper uptake, while exposure to acidic solutions followed by DI water resulted in more relaxed, less charged PAA chains that resulted in larger pore diameters and minor copper uptake. This hysteresis was shown to repeatable and long-lived through continued permeability and copper adsorption experiments.

DOI: 10.1021/jacs.6b01618
J. Am. Chem. Soc. 2016, 138, 7030−7039

FTIR studies demonstrated that the PAA had different levels of ionization in DI water depending on the previous solution in which it had been soaked, and these multiple stable ionization levels imparted the hysteretic physiochemical properties to the polymer. The effect of polymer−polymer hydrogen bonds within the confined nanopores is the most likely source of the hysteresis, with the bonds forming under acidic conditions that held the pores in a stable open state. This is because experiments with urea, which disrupts hydrogen bonds, showed a shift toward the equilibrium, highly ionized form of the confined PAA chains, supporting the mechanism of hydrogen bonding as the cause of the hysteresis. This new understanding regarding the underlying phenomena that control hysteretic behavior in these types of materials provides a unique outlook and a novel approach to macromolecular design of potential materials for sensors and gating processes.

■ ASSOCIATED CONTENT

Supporting Information

The Supporting Information is available free of charge on the ACS Publications website at DOI: 10.1021/jacs.6b01618.

Detailed descriptions of the experimental protocols implemented and materials utilized; chemical structure of PI-PS-PAA, pore diagram of self-assembled surface, and scanning electron micrograph of membrane surface; sample FTIR spectrum showing characteristic peaks; plot of hydraulic permeability as a function of observed degree of ionization; plot of degree of ionization as a function of solution pH from FTIR and copper uptake experiments; plot of copper uptake as a function of observed degree of ionization; method of calculating percent ionizations plotted in Figure S4 from copper uptake experiments; and description and discussion of copper uptake experiments performed for intermediate PAA ionization levels, as shown in Figure 4a. (PDF)

■ AUTHOR INFORMATION

Corresponding Author

*wphillip@nd.edu

Notes

The authors declare no competing financial interest.

■ ACKNOWLEDGMENTS

Portions of this work were made possible with support from the Army Research Office (ARO) through the Polymer Chemistry Program (Award Number: W911NF-14-1-0229, Program Manager: Dr. Dawanne Poree) and the National Science Foundation (NSF) through the Interfacial Processes and Thermodynamics Program (Award Number: 1511835, Program Manager: Dr. Nora Savage), and we appreciatively acknowledge this support. B.W.B. thankfully acknowledges support from the Ralph W. and Grace M. Showalter Research Trust Award at Purdue University. W.A.P. gratefully acknowledges support from the 3M non-Tenured Faculty Award. We would like to thank the Notre Dame Integrated Imaging Facility (NDIIF) and the Center for Environmental Science and Technology (CEST) at Notre Dame; portions of this research were performed with instruments at these facilities.

■ REFERENCES

(1) Stuart, M. A. C.; Huck, W. T. S.; Genzer, J.; Muller, M.; Ober, C.; Stamm, M.; Sukhorukov, G. B.; Szleifer, I.; Tsukruk, V. V.; Urban, M.; Winnik, F.; Zauscher, S.; Luzinov, I.; Minko, S. *Nat. Mater.* **2010**, *9*, 101−113.

(2) Silva, J. M.; Caridade, G.; Costa, R. R.; Alves, M.; Groth, T.; Picart, C.; Reis, R. L.; Mano, F. *Langmuir* **2015**, *31*, 11318−11328.

(3) Nunes, S. P.; Behzad, A. R.; Hooghan, B.; Sougrat, R.; Karunakaran, M.; Pradeep, N.; Vainio, U.; Peinemann, K.-V. *ACS Nano* **2011**, *5*, 3516−3522.

(4) Sugnaux, C.; Lavanant, L.; Klok, H. *Langmuir* **2013**, *29*, 7325−7333.

(5) Hegewald, J.; Schmidt, T.; Eichhorn, K.; Kretschmer, K.; Kuckling, D.; Arndt, K.; Dresden, D. *Langmuir* **2006**, *22*, 5152−5159.

(6) Beltran, S.; Baker, J. P.; Hooper, H. H.; Blanch, H. W.; Prausnitz, J. M. *Macromolecules* **1991**, *24*, 549−551.

(7) Tan, W. S.; Cohen, R. E.; Rubner, M. F.; Sukhishvili, S. A. *Macromolecules* **2010**, *43*, 1950−1957.

(8) Liu, H.; Li, Y.; Sun, K.; Fan, J.; Zhang, P.; Meng, J.; Wang, S.; Jiang, L. *J. Am. Chem. Soc.* **2013**, *135*, 7603−7609.

(9) Chen, Y.; Zhao, T.; Wang, B.; Qiu, D. *Langmuir* **2015**, *31*, 8138−8145.

(10) Annaka, M.; Tanaka, T. *Nature* **1992**, *355*, 430−432.

(11) Itano, K.; Choi, J.; Rubner, M. F. *Macromolecules* **2005**, *38*, 3450−3460.

(12) Hiller, J.; Rubner, M. F. *Macromolecules* **2003**, *36*, 4078−4083.

(13) Lee, D.; Nolte, A. J.; Kunz, A. L.; Rubner, M. F.; Cohen, R. E. *J. Am. Chem. Soc.* **2006**, *128*, 8521−8529.

(14) Secrist, K. E.; Nolte, A. J. *Macromolecules* **2011**, *44*, 2859−2865.

(15) Xiang, T.; Tang, M.; Liu, Y.; Li, H.; Li, L.; Cao, W.; Sun, S.; Zhao, C. *Desalination* **2012**, *295*, 26−34.

(16) Sun, G.; Senapati, S.; Chang, H. *Lab Chip* **2016**, *16*, 1171−1177.

(17) Zhang, H.; Ito, Y. *Langmuir* **2001**, *17*, 8336−8340.

(18) Choi, J.; Rubner, M. F. *Macromolecules* **2005**, *38*, 116−124.

(19) Phillip, W. A.; Dorin, R. M.; Werner, J.; Hoek, E. M. V; Wiesner, U.; Elimelech, M. *Nano Lett.* **2011**, *11*, 2892−2900.

(20) Geismann, C.; Tomicki, F.; Ulbricht, M. *Sep. Sci. Technol.* **2009**, *44*, 3312−3329.

(21) Cho, Y.; Lim, J.; Char, K. *Soft Matter* **2012**, *8*, 10271−10278.

(22) Shi, Q.; Su, Y.; Ning, X.; Chen, W.; Peng, J.; Jiang, Z. *J. Membr. Sci.* **2010**, *347*, 62−68.

(23) Himstedt, H. H.; Du, H.; Marshall, K. M.; Wickramasinghe, S. R.; Qian, X. *Ind. Eng. Chem. Res.* **2013**, *52*, 9259−9269.

(24) Dugdale, D. *Essentials of Electromagnetism*; American Institute of Physics: New York, 1993.

(25) Israelachvili, J. N. *Intermolecular and Surface Forces*, 3rd ed.; Academic Press: Burlington, 2011.

(26) Ch'ng, L. C.; Samanta, A. K.; Czako, G.; Bowman, J. M.; Reisler, H. *J. Am. Chem. Soc.* **2012**, *134*, 15430−15435.

(27) Jung, A.; Filiz, V.; Rangou, S.; Buhr, K.; Merten, P.; Hahn, J.; Clodt, J.; Abetz, C.; Abetz, V. *Macromol. Rapid Commun.* **2013**, *34*, 610−615.

(28) Pendergast, M. M.; Mika Dorin, R.; Phillip, W. A.; Wiesner, U.; Hoek, E. M. V. *J. Membr. Sci.* **2013**, *444*, 461−468.

(29) Peinemann, K.-V.; Abetz, V.; Simon, P. F. W. *Nat. Mater.* **2007**, *6*, 992−996.

(30) Zhang, Y.; Sargent, J. L.; Boudouris, B. W.; Phillip, W. A. *J. Appl. Polym. Sci.* **2015**, *132*, 41683−41699.

(31) Epps, T. H.; Cochran, E. W.; Hardy, C. M.; Bailey, T. S.; Waletzko, R. S.; Bates, F. S. *Macromolecules* **2004**, *37*, 7085−7088.

(32) Bates, F. S.; Fredrickson, G. H.; Bates, F. S.; Fredrickson, G. H. *Phys. Today* **1999**, *52*, 32.

(33) Phillip, W. A.; Rzayev, J.; Hillmyer, M. A.; Cussler, E. L. *J. Membr. Sci.* **2006**, *286*, 144−152.

(34) Phillip, W. A.; O'Neill, B.; Rodwogin, M.; Hillmyer, M. A.; Cussler, E. L. *ACS Appl. Mater. Interfaces* **2010**, *2*, 847−853.

(35) Karunakaran, M.; Nunes, S. P.; Qiu, X.; Yu, H.; Peinemann, K.-V. *J. Membr. Sci.* **2014**, *453*, 471−477.

(36) Mulvenna, R. A.; Weidman, J. L.; Jing, B.; Pople, J. A.; Zhu, Y.; Boudouris, B. W.; Phillip, W. A. *J. Membr. Sci.* **2014**, *470*, 246−256.

(37) Weidman, J. L.; Mulvenna, R. A.; Boudouris, B. W.; Phillip, W. A. *Langmuir* **2015**, *31*, 11113−11123.

DOI: 10.1021/jacs.6b01618
J. Am. Chem. Soc. 2016, 138, 7030−7039

(38) Mihai, I.; Addiego, F.; Ruch, D.; Ball, V. *Sens. Actuators, B* **2014**, *192*, 769−775.
(39) Jayant, K.; Auluck, K.; Funke, M.; Anwar, S.; Phelps, J. B.; Gordon, P. H.; Rajwade, S. R.; Kan, E. C. *Phys. Rev. E* **2013**, *88*, 1−13.
(40) Mulvenna, R. A.; Prato, R. A.; Phillip, W. A.; Boudouris, B. W. *Macromol. Chem. Phys.* **2015**, *216*, 1831−1840.
(41) Germack, D. S.; Wooley, K. L. *J. Polym. Sci., Part A: Polym. Chem.* **2007**, *45*, 4100−4108.
(42) Bates, F. S. *Annu. Rev. Phys. Chem.* **1990**, *41*, 525−557.
(43) Taylor, W.; Jones, R. A. L. *Langmuir* **2010**, *26*, 13954−13958.
(44) Bird, B. B.; Stewart, W. E.; Lightfoot, E. N. *Transport Phenomena*, 2nd ed.; John Wiley and Sons: New York, 2002.
(45) Hautojarvi, J.; Kontturi, K.; Nasman, J. H.; Svarfvar, B. L.; Viinikka, P.; Vuoristo, M. *Ind. Eng. Chem. Res.* **1996**, *35*, 450−457.
(46) Ito, Y.; Kotera, S.; Inaba, M.; Kono, K.; Imanishi, Y. *Polymer* **1990**, *31*, 2157−2161.
(47) Ito, Y.; Inaba, M.; Chung, D.; Imanishi, Y. *Macromolecules* **1992**, *25*, 7313−7316.
(48) Riddick, J. A.; Bunger, W. B.; Sakano, T. K. *Techniques of Chemistry*, 4th ed.; John Wiley and Sons: New York, 1985.
(49) Tagliazucchi, M.; Azzaroni, O.; Szleifer, I. *J. Am. Chem. Soc.* **2010**, *132*, 12404−12411.
(50) Emeis, C. A. *J. Catal.* **1993**, *141*, 347−354.
(51) Rzayev, J.; Hillmyer, M. A. *J. Am. Chem. Soc.* **2005**, *127*, 13373−13379.
(52) Tagliazucchi, M.; Azzaroni, O.; Szleifer, I. *J. Am. Chem. Soc.* **2010**, *132*, 12404−12411.
(53) Wijeratne, S.; Bruening, M. L.; Baker, G. L. *Langmuir* **2013**, *29*, 12720−12729.
(54) Annenkov, V. V.; Danilovtseva, E. N.; Saraev, V. V.; Mikhaleva, A. I. *J. Polym. Sci., Part A: Polym. Chem.* **2003**, *41*, 2256−2263.
(55) Kuntz, I. D.; Brassfield, T. S. *Arch. Biochem. Biophys.* **1971**, *142*, 660−664.
(56) Perry, S. L.; Leon, L.; Hoffman, K. Q.; Kade, M. J.; Priftis, D.; Black, K. A.; Wong, D.; Klein, R. A.; Piercelll, C. F.; Margossian, K. O.; Whitmer, J. K.; Qin, J.; de Pablo, J. J.; Tirrell, M. *Nat. Commun.* **2015**, *6*, 6052−6060.

DOI: 10.1021/jacs.6b01618
J. Am. Chem. Soc. 2016, 138, 7030−7039